On Wavelets

By Nikeet Pandit

ESS 5010

Professor Pagiatakis

Table of Contents

Introduction

In time series analysis, investigation of a series' spectral components is useful tool when the series is sampling a physical phenomenon that is periodic in nature. It is typical then that there are some dominant periodic constituents, usually which are well-studied, that obscure hidden features, which tend to be of interest to researchers since they contain some physical information that is yet to be studied. The former may be referred to as the noise while the later may be referred to as the signal, defined with respect to the researcher's interest. An example of this may be seen when inspecting GRACE-FO's non-gravitational accelerometer data, subjected to powerful constituents from the spacecraft orbital period and its harmonics. Removing these effects reveals a signal where perhaps, localized anomalies attributed to electromagnetic flow of energy may be studied.

Provided the signal is stationary and equally spaced, thus satisfying strict Fourier's requirements, Fourier decomposition is an adequate tool to characterize the signal spectrally, representing the signal efficiently, by showcasing spectral variance. When these assumptions are violated as is the case for most non-idealized signals, or when a researcher has an associated weight matrix for the data-set, the least-squares spectral analysis (LSSA) is a tool that may then provide an undistorted spectral image of the signal that does not require modifying the signal of interest (Wells et at., 1985). Both Fourier and LSSA methods represent spectral constituents as global features of the signal, thereby do not have the capability to provide any time localization. Therefore, when the signal has not reached statistical equilibrium, characterization of the signal to spectral features of interest requires both frequency and time localization.

However, there is a limitation to achieving absolute resolution in both time and frequency domains simultaneously (Keller, 2004). In the limiting case, if we use a delta function as an operational tool to select one value of the signal (Jenkins and Parzen, 1968), absolute time resolution will be realized since we know exactly the amplitude the selected sample takes at the arbitrary time instant. In the frequency domain, however, this corresponds to convolution of the spectrum with a constant, thereby providing no frequency resolution. In the other limiting case, when the window to which we compute the spectrum is the length of the signal, this will tend to the Fourier transform as the signal length approaches infinity, thus offering complete frequency resolution at expense of time resolution. This is known as the uncertainty principal which represents the intrinsic trade-off of achieving frequency and time resolution simultaneously (Brunton and Kutz, 2019).

Wavelet analysis is then a signal processing tool which tries to overcome this principal by using variably-sized windowing lengths for spectrum computation inversely proportional to frequency (Brunton and Kutz, 2019). In effect, wavelets provide multi resolution frequency information across varying time scales, thus providing time and frequency localization simultaneously. More generally, wavelet analysis allows for the characterization of non-stationary signals in the time-frequency domain. Thus, the wavelet transform is useful representation of the signal on a basis which may highlight localized signal constituents with transient amplitude and spectral characteristics (Ghaderpour and Pagiatakis, 2017). For unequally spaced series, Fourier-based wavelet transforms are not defined. Extending the LSSA, in conjunction with the windowing of the wavelet transform, the least-squares wavelet analysis (LSWA) is then a suitable tool for characterization of non-stationary signals when gaps are present (Ghaderpour and Pagiatakis, 2017).

To gain insight into wavelets, a theoretical treatment for Fourier-based wavelet transforms and LSSA-based wavelet transform will be provided, the latter being referred to as Least-Squares Wavelet Analysis (LSWA) with discussion on computational implementation. Thereafter, several investigations will be performed taking form of independent mini-projects. It is with intent that these decoupled investigations will provide meaningful insights to applied application of wavelet analysis when performing experimental analysis in research. The following investigations will be discussed: (1) Matched filtering; (2) Synthetic series testing with comparison of Fourier wavelets and least-squares wavelets; (3) 2D multi-resolution in wavelets for analysis of gravitational gradients.

1. Principle of Wavelets

1.1 Fourier Wavelets

The mathematical wavelet definition of the continuous wavelet transform is written as (Brunton and Kutz, 2019):

$$\gamma(a,b) = \int_{-\infty}^{\infty} f(t)\psi_{a,b}^{*}(t)dt$$

where * signifies complex conjugate. This equation looks very similar to Fourier transform, since the signal is weighted by a set of basis functions. Unlike Fourier transform, which specifies the basis to be cosine and sine, the basis $\psi_{a,b}$ is simply scaled and translated versions of one "mother wavelet" function $\psi(t)$. $\psi_{a,b}$ is defined below, where a and b denote scaling and translating, respectively:

$$\psi_{a,b} = \frac{1}{\sqrt{a}}\psi\left(\frac{t-b}{a}\right)$$

Therefore, the wavelet transform defines the framework for the representation of a signal onto a new basis but does not explicitly define the basis themselves. The $1/\sqrt{a}$ factor is to preserve the area under the wavelet as they are dilated (Valens, 1999). As the wavelet transforms the signal $f(t)$ to a function of scaling and translation, it gives indication on how the transform can provide time and frequency localization simultaneously. Hence, a 1D signal has a 2D transform and so on. The "mother wavelet" function must obey several conditions. First, it must satisfy the admissibility condition which has some interesting implications (Keller, 2004), stating that the Fourier transform of the function must be square integrable and bounded. Since the integral is bounded, as ω tends to zero, $|\psi(\omega)|^2$ must tend to zero also. Since the DC term of the function is $\psi(t)$ is zero, its mean must be zero. Therefore, the function must be oscillatory, and also possesses a band-pass spectrum (Keller, 2004).

With increasing scale, wavelets are stretched in time to find general signal characteristics, while compressing the wavelet is used to find localized detail characteristics. It must be noted that the inverse of wavelet scale and Fourier frequency are different but can be related analytically specific to the wavelet function used (Torrence and Compo, 1998). As such, when plotting a scalogram using a software program, it is incorrect to label the y-axis as frequency unless the software simplicity does this conversion, or the conversion from wavelet scale to Fourier frequency is done explicitly by the user. As noted, the Fourier transform mother wavelet, $\psi(w)$, has a spectrum of a band-pass kernel. Increasing the wavelet scale results

in time, inversely proportional compression of the bandwidth in frequency, as well as the center frequency shifting toward lower frequency. The opposite is true for decreasing scale. This highlights further the uncertainty principal discussed in the introduction. As a result, the mathematical wavelet transform in its continuous form thus requires weighting by an infinite and continuously translated and scaled mother wavelet function to cover the whole spectrum, or equivalently, infinitely many band-pass filter kernels, since they continuously compress with increasing scales.

In practical implementation, there is a low-pass filter which is referred to as the scaling function, "father wavelet", or approximation coefficient, in conjunction to the series of band-pass filters. There are also conditions placed on the smoothness of the function, and restrictions posed on how compacted $\psi(w)$ is in both time and frequency domains. These are known as the regularity conditions (Valens, 1999). The compactness can be described by the number of vanishing moments of the wavelet. Heuristically, it has been experimentally seen that wavelets with more vanishing moments can represent more sparsely a signal by its wavelet coefficients, meaning many of its coefficients will be near-zero. This has practical applications for data compression and data denoising, where an input signal has been subjected to white noise, and where the denoising procedure would like to preserve sharp edge details in the denoised signal. This is confirmed in the publication (Patilkulkarni et al., 2013) and a mathematical treatment is given in (Keller, 2004). A great discussion on practical considerations when choosing the wavelet filter dependent on application and with respect to the amount of vanishing moments is given in (Percival and Walden, 2000), which will serve as a great resource for future work.

Now, the algorithms will be discussed in their computational implementation. Fourier-based wavelet transforms differ in how the scale parameter is discretized (MathWorks). The discrete wavelet transform (DWT) is a completely orthogonal transform meaning the basis for which the signal is projected is linearly independent, while the continuous wavelet transforms (CWT) as coded is highly redundant. The former transform is evidently better suited for compression purposes, while the latter is more tailed for signal analysis at the expense of computational complexity. For DWT as shown in figure 1 retrieved from (Barros, 2012), it is implemented computationally without wavelets at all. In fact, it is implemented through a cascading bank of filters, where the scale discretization is taken to be powers of 2^j, j = 1, 2, 3, … known as the octaves. After each level of decomposition, the DWT down samples by 2, valid based on the Nyquist condition to not introduce aliasing for sparse representation of the signal. The DWT, unlike the CWT, is not shift-invariant and will introduce phase shifts to decomposed results variable to the filter used. To remedy this, a non-decimated version of the DWT, known as the maximum overlap discrete wavelet transform (MODWT), has been introduced with the benefit of being shift-invariant and associated with zero-phase filters, meaning decomposed features can be lined up with the original signal without deflection. While not studied in this report, future work will investigate the MODWT.

For the CWT, in MATLAB for example, powers of 2 are also taken as the doubling factor, however, it also samples at 10 (by default) intermediate scales between subsequent powers, known as sub-octaves (see MathWorks documentation) which achieves a finer scalogram result. Hence, for both CWT and DWT, higher levels of decomposition refer to lower frequency constituents.

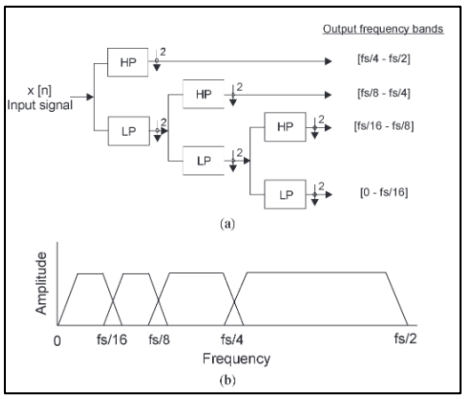

Figure 1

From the way this discretization is being performed using powers of 2 for both the CWT and DWT, even considering the fact that the user has the ability to parameterize the number of sub-octaves, towards high frequencies, time resolution is worse than inversely related to frequency resolution. In effect, it is non-linear with an exponential of base 2, which may be offset by the level of sub-octaves, depending on if the DWT or CWT is used. However, the offsetting cannot be so great to offset the non-linear effect of the logarithmic scale without being impractical to implement computationally. Theoretically, we should expect an inverse relationship between time resolution and frequency trade off, however, to the writer's knowledge it is not possible to change the base of discretization for the scale in the several Fourier-based wavelet transform algorithms tested. This is perhaps why in MATLAB by default, the CWT plots in logarithmic scale to smooth the grainy effect toward higher frequencies. From here we note, the inefficacy of these algorithms for signal analysis when fidelity is a chief concern.

1.2 Least-Squares Wavelets

Similar to the CWT, the LSWA is also a highly redundant transform geared toward signal high fidelity signal analysis. The theory from the LSWA is treated thoroughly in (Ghaderpour and Pagiatakis, 2017) and the software was written by Dr Ghaderpour. The LSWA has the great benefit over the CWT in that it is very easy to parameterize effectively the desired time frequency resolution in the scalogram. In effect, the LSWA computes varied size windows as a function of three user-defined parameters, where for each window, the LSSA spectrum is computed. Since the LSSA is defined for gappy series, as well allowing for a weighting matrix as input, the LSWA will evidently permit this as well, representing another key benefit of the LSWA over the CWT. Windows are analogous to scales in the CWT. Since the series may be gappy, a window for a given size is fixed with respect to the samples resolved with in it for the LSSA computation, not its length. Hence, its length may vary accordingly to the irregularity of the sampling of the series. In an equisampled series, the length is equivalent to the size, scaled by the sampling rate. The function that determines the window size, or the number of samples resolved in each window for LSSA computation is defined below,

$$L(\omega_k) = \left\lceil \frac{L_1 M}{\omega_k} \right\rceil + L_0$$

if the number of samples is odd. If the number of samples is even, an additional sample is taken. From here, we note that if $L_1 = 0$, for some $L_0 > 0$, the window length then remains fixed irrespective of frequency and resembles the Gabor transform. When $L_1 > 0$ we can see, scaled by the sampling rate M, the window length is inversely proportional to the frequency, analogous to the CWT. From here, we note that L_0 is then a fixed number of additional samples to include in the resolved samples for the LSSA calculation. This factor allows the user to parameterize time-frequency resolution desired, which may be tailored to the analysis. Evidently, larger values will increase frequency resolution at cost of time resolution and vice versa, so parameterization then depends on quickness of the transient constituents of the signal. However,

it is noted in (Ghaderpour and Pagiatakis, 2017), that when using large L_0 for a very gappy series, the window length may vary significantly for a given scale. This may attenuate significantly in the spectrogram a very localized, transient signal. The LSSA nominally uses cosine and sine basis functions, and thus LSWA uses sinusoids as its basis. However, since any basis function may be defined for the LSSA, the user is not constrained to these base functions. As programmed, the user may select to weight the sinusoids with a gaussian function. In effect, this weighting procedure results in Morlet basis. In the software, the user can parameterize the Morlet constant. A larger magnitude constant results in a smoother spectrogram at the cost of worse frequency resolution and vice versa. This can be summarized by the bias-variance trade off.

2. Methodology

2.1 Matched Filtering

Matched filtering refers to the location of a known embedded signal that is obscured by noise. In this experiment, the Mexican hat function, or second derivative of a Gaussian function, will be placed in a series of white noise. Two methods will be compared against.

2.1.1 Correlation Filter

When the noise is white, correlating the total noise and signal with the known signal, is an optimal method since the peak of correlation is greater than the noise floor, when compared to any other linear filter (Smith, 2003). For this matched filter, we take the impulse function to be the known Mexican hat function and convolve this with the signal and noise. Since the hat function is symmetrical, this operation is identical to computing the cross correlation between the two signals.

2.1.2 LSWA with Adapted Basis

In another attempt to locate the hat function, the LSWA was used. Since the LSWA computes fractionally, in the least-squares sense, the content of the windowed signal which can be represented by the base functions, the LSWA should theoretically provide some advantages over the correlation filter (Wells et al., 1985). Most notably, the exact width of the signal need not be known, except its general structure. This is predicated on the basis for which the LSWA is computed perhaps be changed to match the signal. As such, implementing a feature in the LSWA to a Mexican hat basis, in place of the sinusoid basis that is nominally implemented would surely be beneficial. The methodology to do this is now explained. First, the normalized Mexican hat distribution is defined

$$\psi(t) = \frac{2}{\sqrt{3}\pi^{\frac{1}{4}}}\left(1 - \left(\frac{t-\mu}{\sigma}\right)^2\right)e^{-\frac{(t-\mu)^2}{2\sigma^2}}$$

Since the distribution is completely specified by μ and σ^2, it will be referred by ~$N(\mu, \sigma^2)$. For each translated window of varying length, the Mexican hat distribution will be a scaled and translated unit distribution evaluated at the windowed time vector. The unit distribution, for which all distributions will be scaled and translated versions of, is defined as $X = N(0,1)$ and will be evaluated for $5 \leq t \leq 5$ since this interval contains nearly 100% of the distribution energy. We can then let scaled and translated functions of X be denoted by $Y = aX + b$. The new distribution, defined by $Y = N(\mu_2, \sigma_2^2)$ is then a function of Y where $\mu_2 = a\mu_1 + b$ and $\sigma_2^2 = a^2\sigma_1^2$ where $\mu_1 = 0$ and $\sigma_1^2 = 1$.

b, the translation, is found as the median of the time vector. In the LSWA, a condition was placed to ensure the time vector is odd, so that there would be even elements on each side of the median, ensuring a symmetrical Y. The scale a was determined as a function the windowed time vector $a = \sqrt{t(end) - b/5}$ where $t(end)$ denotes the final element of the time vector. There is a division by 5 since the unit distribution X is evaluated over the interval $5 \leq t \leq 5$. By determining the scale a, there is no adjustment that needs to be made when computing the LSWA on the user-side, except of course, a different interpretation of the parameterization of the software, namely the L0, L1, and omega values.

2.1.3 Testing Procedure

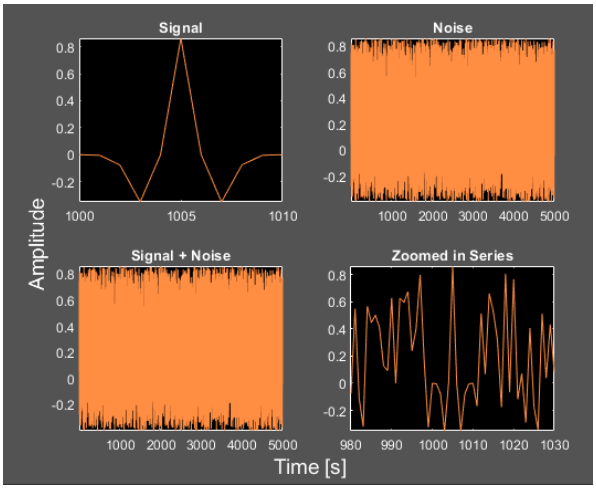

Figure 2

The noise, signal, signal and noise are shown in figure 2. Three signals of 10 second duration are distributed throughout the signal. One at the 1000s, another at 2000s, and the final at 4000s. The amplitude of the signal and the noise are also approximately the same. Upon investigation of the signal + noise figure, visually it is not identifiable where the signal is located. Evidently, the noise is very strong and obscuring the signal. The difficulty of this experiment arises by the fact that a Mexican hat function can resemble the random variability of white noise.

2.2 Wavelet Analysis on Synthetic

In this segment, testing methodology will comprise wavelet analysis by the LSWA with sinusoid basis, and the CWT. First we will contrast LSWA and CWT using two hyperbolic chirp signals, similar to what was performed in (Ghaderpour and Pagiatakis, 2017). Different conclusions will be drawn, since (Ghaderpour and Pagiatakis, 2017) did not incorporate the usage of the stochastic surface, whose usage, draws a remarkably different resultant spectrogram. After, the LSWA will be applied to the same series, except the series will be made gappy to see the effect it has on the spectrogram.

2.2.1 Synthetic Series Construction

Equally Spaced Series

Two quadratic chirp functions are constructed individually with added white noise, and then lumped together as shown in figure 3. Both are sampled at $Fs = 1000Hz$ with a duration $T = 0.5s$. The first function starts at 50Hz and reaches 400Hz at 0.5 seconds. The second function starts at 5 Hz and reaches 350 at 0.5 seconds. The plot is appended below. The signal to noise ratio (SNR) is taken to be 40dB.

Gappy Series

The same quadratic chirp series are made gappy by an original *make_gappy* algorithm. The user parses in the original series and probability to make a specific element gappy or not. For this example. probability of

gap is 30%. 137 elements are randomly removed from the 501-length series, corresponding to about 28% removal from the original series. The 2% difference can be attributed to statistical interference.

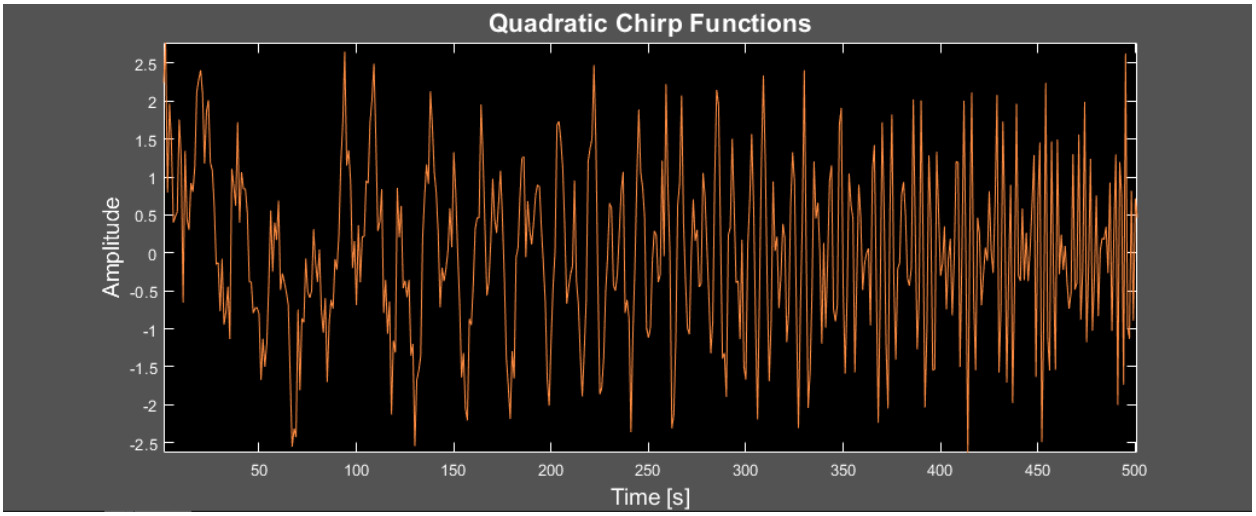

Figure 3

2.3 MRA in 2D

This MRA in 2D theory resembles Nikeet Pandit's Image Processing final project on image compression.

Extending the DWT discussion as provided in the Fourier wavelet theoretical treatment, the 1D transform is easily extended to the 2D case and is treated in (Gonzales and Woods, 2018). Since the DWT is separable, the DWT is simply taken on the columns of the input 2D matrix, followed by the DWT on the resulting rows. Each level of decomposition in the 2D case will give approximation coefficients, and three detail coefficients corresponding to the horizontal, the vertical, and the diagonal (Gonzales and Woods, 2018). These correspond to high frequency variations in the respective directions. If doing a N level decomposition, the detail coefficients may be summed for N-1 levels and for the N^{th} level, the approximation coefficients is also summed with the detail coefficients, as discussed in (Peidou, 2020). Since for the DWT, the algorithm downsamples after each level of decomposition, for visualization, Sinc interpolation is performed since it provides perfect reconstruction of a band-limited signal (Jenkins and Parzen, 1968). 11 levels of decomposition are used as well as the Daubechies wavelet of order 2 to perform multi-resolution analysis (MRA). More work needs to be done in investigation on wavelet order and family and its effect on the MRA. Applying the original algorithm to a test case, a gravitational gradient model, GGM05S, is downloaded from GFZ in the radial direction with respect to the ellipsoid over the Indonesia area.

3. Results and Discussion

3.1 Matched Filtering

3.1.1 Correlation Filter

Employing cross correlation matched filter result, as seen in figure 4, the location of the signal cannot be detected from the filter result since the correlation also resembles white noise.

3.1.2 LSWA with Adapted Basis

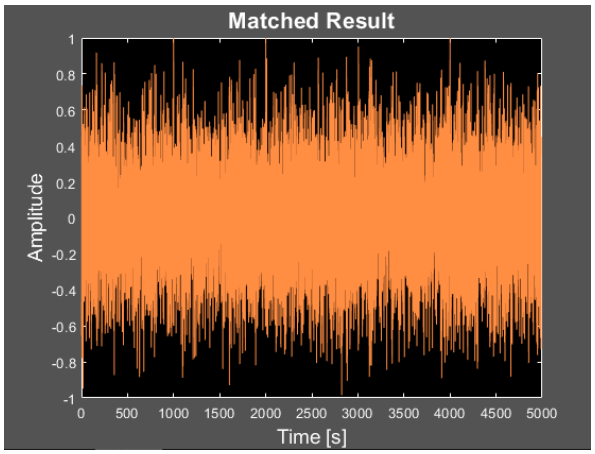

Figure 4

The LSWA proved to be very promising for matched filtering, relative to the correlation filter as it locates exactly the signals embedded in the noise with very good indication of the duration of the signal since the percentage variance is highest at the location of the signals. Only the statistically significant peaks in the spectrogram with 99% confidence is shown. Without use of the stochastic surface, no information can be inferred from the spectrogram. The three streaks in red, corresponding to nearly 100% percentage variance in the spectrogram, when viewed with respect to the time axis, correspond exactly to the time in seconds of where the signal is placed in noise. The signal length, as viewed from signal length axis in the spectrogram, is between 9-11 seconds which exactly comprises the 10 second signal duration. There are three streaks of very low power percentage variance, between signal lengths of 21 and 33 seconds, which can be attributed to the white noise structure having some resemblance to the Mexican Hat signal at those instances.

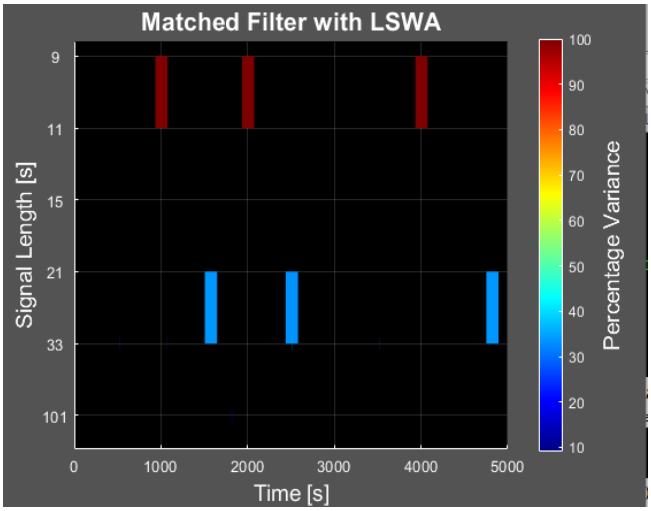

Figure 5

More rigid testing has been done and the signal can be detected in longer length series without knowledge of where they are placed and only with general knowledge of its duration, where the windowing LSWA accounts for uncertainty in signal duration length. In addition to be able to locate the signal, the LSWA matched filter also provides these benefits over the correlation matched filter. While the Mexican Hat function also resembles a very compressed sine wave, performing the LSWA to detect the signal with a sinusoidal basis does not locate the signal with the same efficacy even with very high-resolution analysis since the white noise also resembles compressed sine waves so the end result is large percentage variance everywhere even with usage of the stochastic surface.

Theoretically, using LSWA with adopted basis equivalent to the signal that is desired to be located should always yield a very respectable result, since fractionally there will be moments where the basis is represented very well when the signal is located, if not exactly depending on the additional noise added to the signal at the moment, with little fractional representation elsewhere, as indicated in figure 5. This writer believes that this method could be used and applied to other basis, for example location of GRACE-FO non-gravitational accelerometer jumps in the total GPS orbit determination result. This is predicated that the basis is derived explicitly from jumps in the non-gravitational accelerometer measurements. The signal length, as labelled in figure 5, was determined from the LSWA by extracting the window length for LSSA computation. A much-needed improvement would be to include direct user-parameterization for

windowing as a function of signal length, as opposed to frequency. This would make the solution a very simple matched filter with high efficacy.

3.2 Wavelet Analysis on Synthetic Series

3.2.1 LSWA vs CWT

On (a) in figure 6, we have the CWT using a Morlet wavelet. As discussed in the theory section concerning the Fourier-based wavelets, MATLAB discretize the scale using powers of 2, with the CWT using sub-octaves to obtain finer resolution compared to the DWT. By default, this value is set to 10, however, for the purpose of analysis the maximum sub-octave level of 48 was used. The effect on the CWT was a

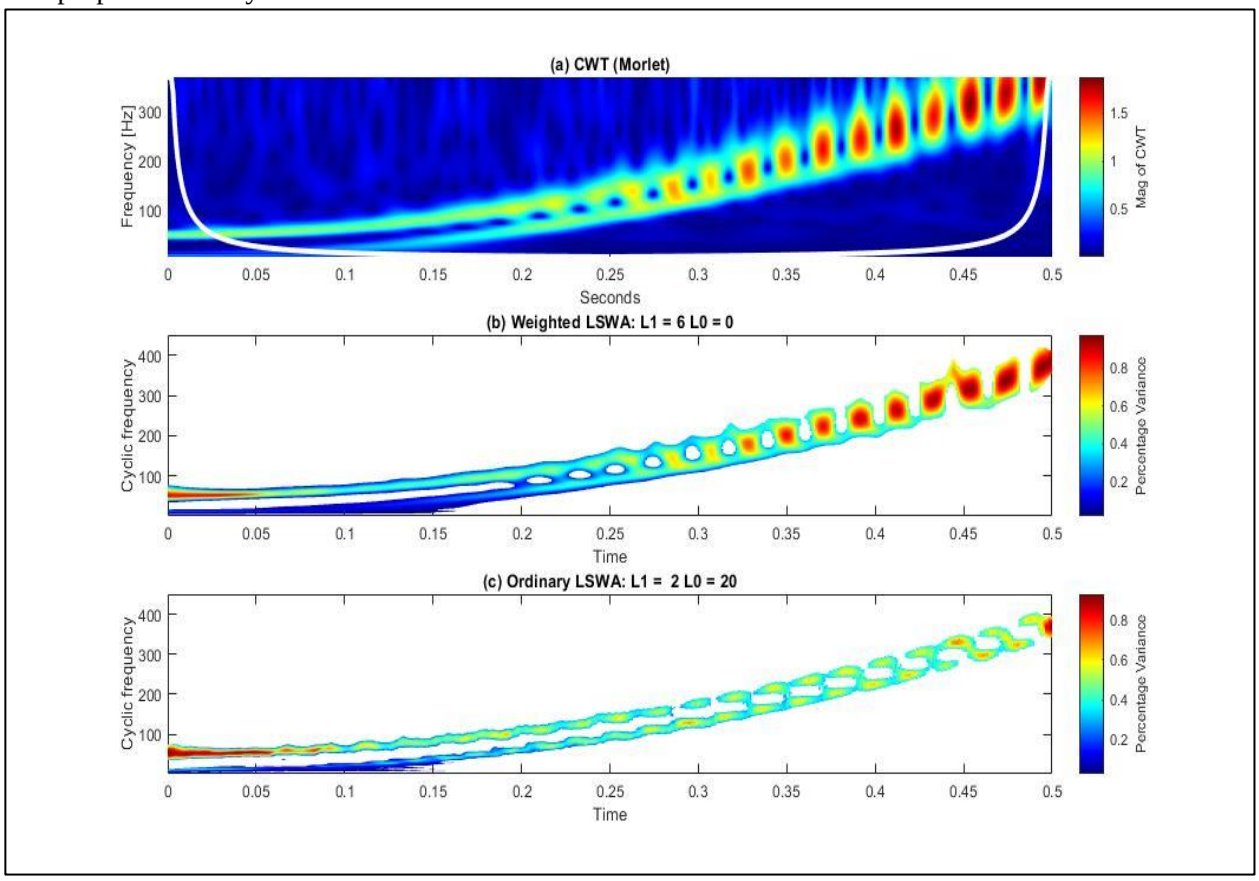

Figure 6

significantly higher resolution spectrogram. As such, if using the CWT for signal analysis, it is highly recommended that this factor be used. We note that around 150 Hz, the two chirp signals cannot be resolved in frequency and begin to merge into one. Interestingly, we see at about 0.33 seconds that the colormap of the spectrogram is showing an increase in magnitude which grows for the rest of the spectrogram. This pattern is repeated in (b), where due to the weighting by a Gaussian function, a Morlet basis is also used. Since there is no variable amplitude in either of the chirp signals, this is an artifact of the spectrogram and perhaps has different reasons for arising in the LSWA compared with the CWT. Theoretically, for the CWT, when a wavelet is compressed to capture shorter-scale (high frequency) features in the signal, its frequency domain counterpart is dilated. This results in a smoothing of peaks in the spectrogram, thereby reducing its

magnitude which can explain also the worse frequency resolution at higher frequencies in (a). To rectify the bias in the estimator, MATLAB uses L1 normalization. Perhaps, this method of regularization slightly over-corrects as frequencies tend to Nyquist. Regardless of the wavelet used, the CWT has this bias for all exhaustive testing performed, which is not limited to what is appended in this report. For these reasons, it suspected that it may be attributed to the L1 regularization. The LSWA, on the other hand, seems to have this bias only when the Morlet weighting function is used. Moreover, when the Morlet smoothing coefficient is lowered from its default value of 0.0125, the bias decreases. Tending the smoothing coefficient to zero, the bias is eliminated almost completely as in (c), except on the edges of the spectrogram. The biases on the edge of the spectrogram can perhaps be attributed to the fact that the boundaries of the series result in non-fully populated windows of samples for the LSSA to be resolved in, known as “marginal windows”.

In both (b) and (c) any constituents in the spectrogram which are deemed not statistically significant, depending on the selected significance level, are turned white which reveals a very clean spectrogram visually. For (b), we see the effect of the Morlet weighting is worse frequency resolution, with the benefit of a slightly smoother spectrogram when compared to (c). The smoothing effect of the Morlet is much more significant when the stochastic surface is not used, as will be shown later in this discussion. When the stochastic surface is used, which essentially has an implicit smoothing characteristic through removal of statistically insignificant noise, the effect of the Morlet is detrimental. Since for the ordinary LSWA in (c), we note that the two chirp signals can almost be completely resolved, with slight overlap occurring around the 0.4 mark. This is a significant improvement over both (a) and (b), also associating correctly 50% percentage to both equal amplitude chirp signals, for the series excluding the boundaries.

Investigating the SNR of the signal, we see that the LSWA performs significantly better than the CWT when the signal is subjected to high noise. Testing a SNR of -1dB and using a statistical confidence level of 90% due to the presence of high noise for LSWA, the results are appended in figure 7. SNR of -2dB is

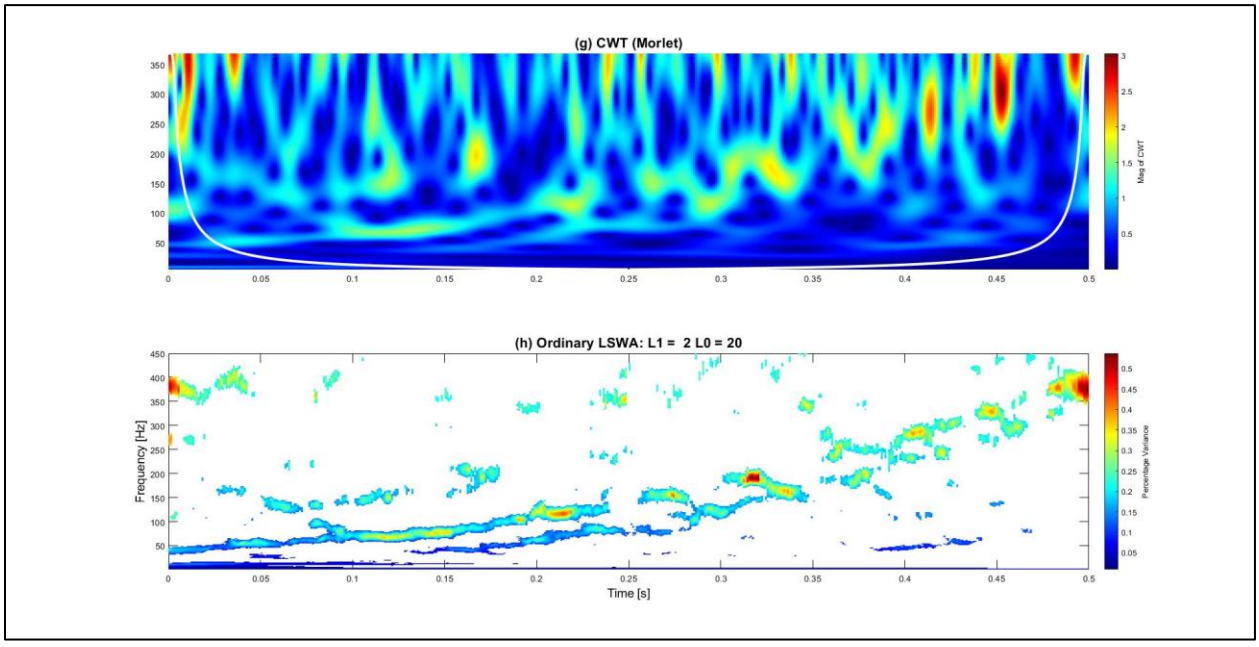

Figure 7

about the lowest the LSWA will allow for resolving the chirp signals, while the CWT is 5dB, since without the stochastic surface, the spectrogram shows significant power everywhere in the spectrogram, as shown in (g).

3.2.2 LSWA Parameterization

To highlight how L0 and L1 are parameterized, we use two extreme cases with great frequency resolution as in (d) in figure 8, and great time resolution shown in (e) and (f), where in (e) the stochastic surface is not used in plotting of the spectrogram. In (d), we select L1 = 40, enforcing 40 cycles of sinusoids being fitted to each window, with no additional samples used, by L0 = 0. We see the practical implication of the uncertainty principal, which was discussed in the introduction, whereby parameterizing greater frequency resolution we lose time localization in the spectrogram indicative of the horizontal smearing across time of

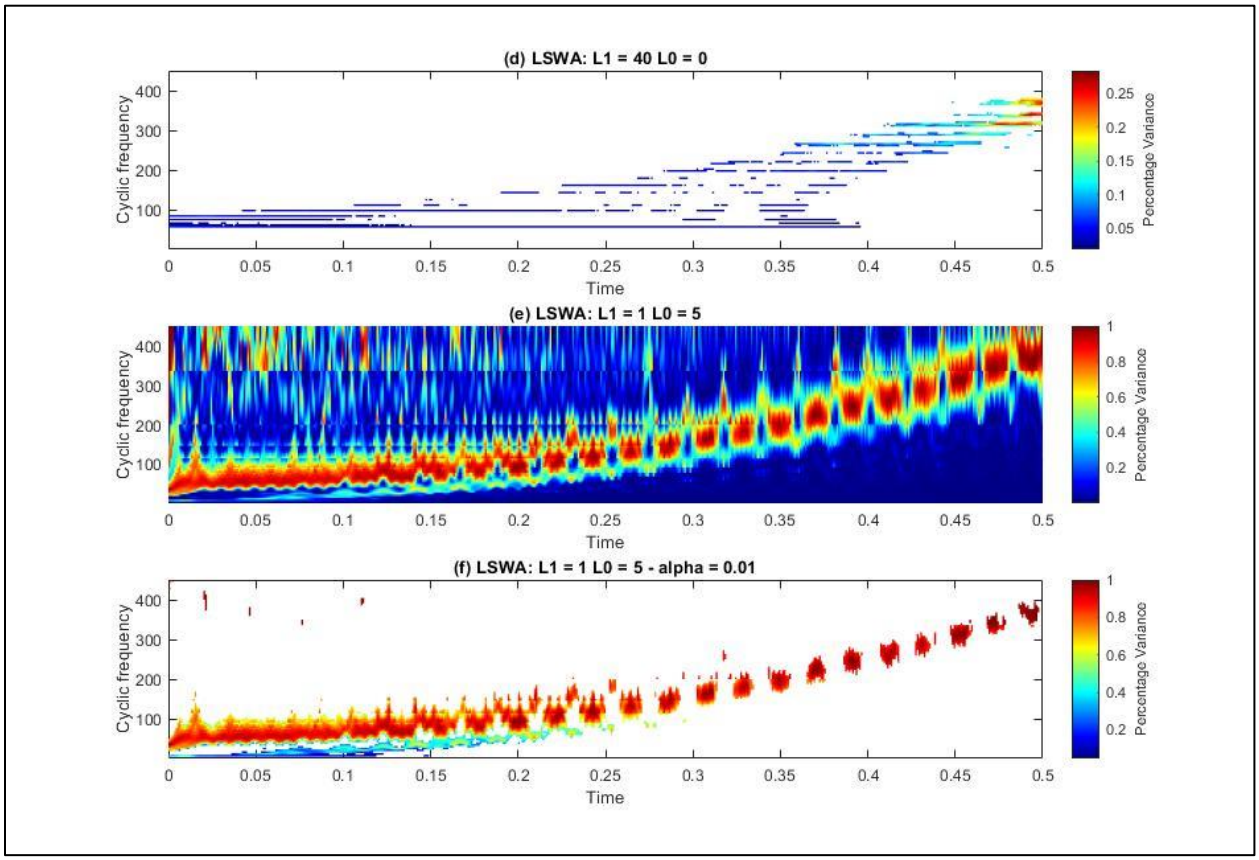

Figure 8

spectral constituents for each given cyclic frequency in Hz. We can tend this result to essentially compute the LSSA for the entire series length at each frequency, corresponding to a spectrum analysis with LSSA. Conversely, in (e), we see the opposite effect where L1 = 1 and L0 = 5, which constructs the absolute smallest window sizes in the LSWA allowable for the synthetic series. In effect, this parameterizes greatest time resolution allowable at expense of frequency resolution. In (Ghaderpour and Pagiatakis, 2017), it notes the presence of these spikes which appear since one cycle of sinusoids can also fit at these horizontal time crossings. Relating to the uncertainty principal again, it seems the effect of absolute time localization is complete loss of frequency resolution, since for every horizontal time crossing, spectral information is

smeared across all frequencies. In (Ghaderpour and Pagiatakis, 2017), Dr Ghaderpour recommends the use of the Morlet to smooth out the presence of these spikes. However, as discussed earlier, the effect of using the stochastic surface effectively removes these spikes in the spectrogram anyway without increasing the bandwidth. Experimentally, it has been seen that stripes in the spectrogram appear if approximately less than 4 cycles of sinusoids, including extra samples, are being fit to the windowed series with the LSSA. We can conclude this analysis to say that stripes appear as a consequence of parameterizing L0 and L1 to provide very high time resolution and is a practical realization of the uncertainty principal. While (Ghaderpour and Pagiatakis, 2017) recommends using the Morlet to smooth the spectrogram, this report advises usage of the stochastic surface which also happens to remove stripes without increasing bandwidth, whose significant level, can also be parameterized based on the scope of the analysis.

3.2.3 LSWA on Gappy

Even with 28% of samples randomly removed from the original series, which itself is actually very short of only 501 samples, using the same parameters as figure 6 (b), and without any modification, the LSWA remarkably shows almost the same spectrogram when applied to the fully populated series. In fact, it actually performs better than the CWT figure 6 (a) which is computed using all the samples.

3.3 MRA in 2D

In figure 9, the MRA in 2D over the Indonesian region is performed based on the methodology described in Section 2.3. In the figure, SH is to denote spherical harmonics and is determined based on the dyadic scale sampling of the DWT. In level 7, we note the general broad characteristics of the total result, in the lower right corner, are well summarized. Investigation of the power distribution, we see there is minimal power for spherical harmonics greater than 128, corresponding to short wavelength features which is expected to the broad-like characteristics of the original map. From this result, we note the efficacy and consistency in result, regardless of mother wavelet, for using the DWT for MRA with respect to investigation of the power distribution of the original scale across varying spatial resolutions.

When using the DWT for investigation of features where accurate spatial localization of the features is essential, as in using DWT for MRA of a gravity functional, the same cannot be said. This is attributed to the downsampling of each subsequent level, lack of shift invariance of the DWT, and phase-distortion causing variable deflection of features on subsequent decomposed levels with respect to the original signal. Therefore, future work will investigate performing the MRA in 2D with the non-decimated version of the DWT, known as the MODWT, which benefits over the nominal DWT in these regards.

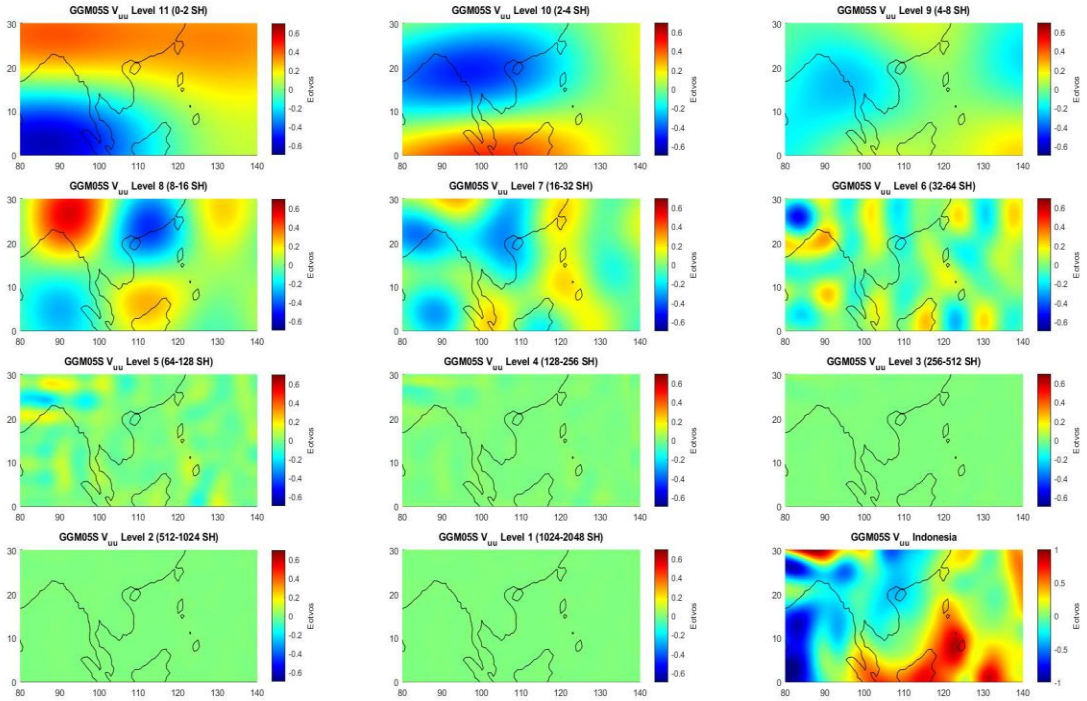

Figure 9

Conclusion

In this report, a wide variety of topics concerning wavelets were discussed. Namely, the reasons for using wavelets were introduced with regard to the uncertainty principal and its benefits over classical spectra analysis. A treatment of both Fourier-based and least-squares wavelets was provided, bridging theoretical ideas to its computational implementation. Three applications were implemented surveying matched filtering, synthetic series testing, and MRA in 2D applied to a gravitational gradient model. To perform matched filtering with the LSWA, a new basis was implemented into the software whose basis was the signal desired to be located in the noise. The robustness of the application was shown which was able to locate the signal embedded in noise with very good time localization and ability to determine, within a very small range, the duration of the signal in the noise where exact duration of the signal, nor location of the signal need not be known. This was an incredible result relative to the optimal matched filter result, which could not detect the signal at all.

In the wavelet analysis on the synthetic series application, exhaustive comparison testing with CWT and LSWA was performed; testing gappy series, variable SNR, and parameterization of the LSWA window parameters. The benefit of using the stochastic surface for the LSWA was also displayed. It was seen at the expense of computational complexity, the LSWA yields a better characterization of the signal in the time-frequency domain. However, since the LSWA computes each spectral component out-of-context, the LSWA would be well suited for parallelization of the algorithm which perhaps could be surveyed in future

work. To display how a user can parameterize the LSWA for desired time-frequency tradeoffs, limiting cases highlighting how the parameters should be set based on the degree of non-stationarity of the series was provided.

The final application was using the DWT for MRA of 2D gravitational gradient map provided by GFZ. It was seen that while the DWT provided a good analysis of the power distribution across varying spatial resolutions, based on the theoretical treatment as provided in this report, the DWT is not useful in location of geophysical signals across the different resolutions due to the lack of shift invariance and phase distortions. Therefore, future work will investigate the MODWT, which does not have these effects, for the analysis of gradient solutions. This project was done with the purpose of setting a solid fundamental for spectral analysis, especially in the context of using wavelets, for experimental research work. By applying rigid testing to synthetic series, experimenting with parametrization, investigating matched filtering, performing 2D MRA in wavelets, and studying deeply theory with links to computational application, it is believed then that this project was successful in achieving this driving goal.

References

Wells D., Vanicek P., Pagiatakis S (1985) Least Squares Spectral Analysis Revisited. University of New Brunswick.

Wolfgang Keller. Wavelets in Geodesy and Geodynamics. Walter de Gruyter; 2004.

Steven L. Brunton, Nathan Kutz. Data-Driven Science and Engineering: Machine Learning, Dynamical Systems, and Control. Cambridge University Press; 2019

Ghaderpour, E. and Pagiatakis, S.D., 2017. Least-squares wavelet analysis of unequally spaced and non-stationary time series and its applications. Math. Geo, 49(7), pp.819-844

C. Valens, 1999. A Really Friendly Guide to Wavelets.

Torrence, G. and Compo G.P., 1998. A Practical Guide to Wavelet Analysis. American Meteorological Society. Vol 79.

Continuous and Discrete Wavelet Transform, MathWorks, last accessed 21 May 2021, https://www.mathworks.com/help/wavelet/gs/continuous-and-discrete-wavelet-transforms.html

S. Smith. 2003. Digital Signal Processing: A Practical Guide for Engineers and Scientists. Newnes.

Wells, D, Vanicek P, Pagiatakis S., 1985. Least Squares Spectral Analysis Revisited. UNB.

Patilkulkarni, S, and H C Vijaylakshmi., 2013. Vanishing Moments of a Wavelet System and Feature Set in Face Detection Problem for Color Images. International journal of computer applications 66.16

D. Percival and A Walden. Wavelet Methods for Time Series Analysis. Cambridge University Press; 2000.

J. Barros. 2012. Applications of Wavelet Transform for Analysis of Harmonic Distortion in Power Systems: A review. IEEE Transactions on Instrumentation and Measurements. V(61).

R. Gonzales, R. Woods. 2018. Digital Image Processing 4ed. Pearson.

Peidou, A., 2020. The New Concept of GRACE Gradiometry and the Unravelling of the Mystery of Stripes. York University.

G. Jenkins and E. Parzen. 1968. Spectral Analysis and its Applications. Holden-Day.